Arteriosclerosis, Thrombosis, and Vascular Biology

JOURNAL OF THE AMERICAN HEART ASSOCIATION

American Heart Association®

Learn and Live℠

Molecular Mechanisms of Atherosclerosis in Metabolic Syndrome : Role of Reduced IRS2-Dependent Signaling

Herminia González-Navarro, Ángela Vinué, Marian Vila-Caballer, Ana Fortuño, Oscar Beloqui, Guillermo Zalba, Deborah Burks, Javier Díez and Vicente Andrés

Arterioscler Thromb Vasc Biol 2008, 28:2187-2194: originally published online September 18, 2008
doi: 10.1161/ATVBAHA.108.175299
Arteriosclerosis, Thrombosis, and Vascular Biology is published by the American Heart Association. 7272 Greenville Avenue, Dallas, TX 72514
 Print ISSN: 1079-5642. Online ISSN: 1524-4636

Molecular Mechanisms of Atherosclerosis in Metabolic Syndrome

Role of Reduced IRS2-Dependent Signaling

Herminia González-Navarro, Ángela Vinué, Marian Vila-Caballer, Ana Fortuño, Oscar Beloqui, Guillermo Zalba, Deborah Burks, Javier Díez, Vicente Andrés

Objective—The mechanisms underlying accelerated atherosclerosis in metabolic syndrome (MetS) patients remain poorly defined. In the mouse, complete disruption of insulin receptor substrate-2 (*Irs2*) causes insulin resistance, MetS-like manifestations, and accelerates atherosclerosis. Here, we performed human, mouse, and cell culture studies to gain insight into the contribution of defective *Irs2* signaling to MetS-associated alterations.

Methods and Results—In circulating leukocytes from insulin-resistant MetS patients, *Irs2* and *Akt2* mRNA levels inversely correlate with plasma insulin levels and HOMA index and are reduced compared to insulin-sensitive MetS patients. Notably, a moderate reduction in *Irs2* expression in fat-fed *apolipoprotein E-null* mice lacking one allele of *Irs2* ($apoE^{-/-}Irs2^{+/-}$) accelerates atherosclerosis compared to *apoE-null* controls, without affecting plaque composition. Partial *Irs2* inactivation also increases CD36 and SRA scavenger receptor expression and modified LDL uptake in macrophages, diminishes *Akt2* and *Ras* expression in aorta, and enhances expression of the proatherogenic cytokine MCP1 in aorta and primary vascular smooth muscle cells (VSMCs) and macrophages. Inhibition of AKT or ERK1/2, a downstream target of RAS, upregulates *Mcp1* in VSMCs.

Conclusions—Enhanced levels of MCP1 resulting from reduced IRS2 expression and accompanying defects in AKT2 and Ras/ERK1/2 signaling pathways may contribute to accelerated atherosclerosis in MetS states. **(*Arterioscler Thromb Vasc Biol.* 2008;28:2187-2194.)**

Key Words: insulin resistance/metabolic syndrome ■ atherosclerosis ■ IRS2 ■ AKT ■ extracellular signal-regulated kinase (ERK)

The metabolic syndrome (MetS) is defined by the presence of at least 3 of the following abnormalities: abdominal obesity, glucose intolerance, hypertension, low HDL-cholesterol levels, or hypertriglyceridemia.[1,2] Patients with MetS and type-2 diabetes mellitus (T2DM) have 2 to 5 times higher risk of atherosclerosis, a chronic inflammatory disease that results from interactions between modified lipoproteins and cells of the arterial wall, including endothelial, immune, and vascular smooth muscle cells (VSMCs).[3–5] Among the different cardiovascular risk factors that precipitate atherosclerosis and associated cardiovascular disease (CVD), T2DM and MetS are becoming the most relevant given that the prevalence of these metabolic diseases is expected to increase by 165% in the next 40 years, representing the health plague of the 21st century.[2] Importantly, the incidence of CVD increases when T2DM and the MetS coexist.[1,2] Population aging and acquisition of sedentary lifestyle patterns (eg, obesity and physical inactivity) are major driving forces behind these metabolic diseases. A number of alterations in endothelial cells, VSMCs, and platelets have been identified which may accelerate atherosclerosis, plaque instability, and thrombus formation in T2DM/MetS patients, however the underlying mechanisms remain ill defined.[2,6,7] Many MetS patients display insulin resistance (IR), which seems to play a pivotal role in the development of both atherogenic dyslipidemia and T2DM.[1] Therefore, IR is an attractive target for prevention of CVD. However, whether IR management per se might reduce CVD risk remains unknown.

On binding to the insulin receptor (INS-R), insulin exerts its action through insulin-receptor substrate proteins (IRS1–4).[8] Studies in genetically-modified mice have highlighted a major role of IRS2 in β-cell function, glucose and insulin homeostasis, and atherosclerosis development. First, *Irs2*-null mice ($Irs2^{-/-}$) display a T2DM/MetS-like phenotype, including hyperglucemia, hyperinsulinemia, IR and hypertension.[9–11] Second, global *Irs2*-deficiency in *apoE*-null mice

Original received April 30, 2008; final version accepted August 30, 2008.

From the Laboratory of Vascular Biology (H.G.-N., A.V., M.V.-C., V.A.), Department of Molecular and Cellular Pathology and Therapy, Instituto de Biomedicina de Valencia, CSIC, Spain; the Division of Cardiovascular Sciences (A.F., O.B., G.Z., J.D.), Centre for Applied Medical Research; Department of Cardiology and Cardiovascular Surgery, University Clinic (J.D.), School of Medicine, University of Navarra, Pamplona, Spain; and the Centro de Investigación Príncipe Felipe (D.B.), CIBER de Diabetes y Enfermedades Metabólicas Asociadas (CIBERDEM), Valencia, Spain.

Correspondence to Vicente Andrés, Instituto de Biomedicina de Valencia, Jaime Roig, 11, Valencia, 46010 Spain. E-mail vandres@ibv.csic.es

Arterioscler Thromb Vasc Biol **is available at http://atvb.ahajournals.org** **DOI: 10.1161/ATVBAHA.108.175299**

($apoE^{-/-}Irs2^{-/-}$) aggravates atherosclerosis compared to $apoE^{-/-}$ counterparts with intact *Irs2*.[12,13] Doubly deficient $apoE^{-/-}Irs2^{-/-}$ mice exhibit hyperinsulinemia, IR, and increased glucose intolerance and a positive correlation between circulating insulin levels and atherosclerotic burden,[12] consistent with findings in $Lep^{ob/ob}$:$LDLr^{-/-}$ and $Lep^{ob/ob}$:$apoE^{-/-}$ mice, two additional models of IR-dependent accelerated atherosclerosis.[14] It is noteworthy that although whole body *Irs2* ablation aggravated atherosclerosis,[12,13] the effects of macrophage-specific defective insulin signaling are controversial. Indeed, *Ins-r*–deficient bone-marrow transplant enhanced atherosclerosis in $LDLr^{-/-}$ mice,[15] however macrophage-specific inactivation of *Ins-r* or *Irs2* decreased atherosclerosis in $apoE^{-/-}$ mice.[13] The reasons for these controversial findings remain to be established.

The two main downstream effectors of IRS proteins are the phosphatidylinositol-3 kinase (PI-3K)/V-akt murine thymoma viral oncogene homolog kinase (AKT) and the Ras/Raf/ERK pathways.[8] Marked reductions in *Ins-r, Irs2*, and *Akt2* gene expression have been reported in pancreatic islets from T2DM patients.[16] Here we have tested the hypothesis that impaired IRS2 signaling is a mechanism contributing to accelerated atherosclerosis in MetS states. To this end, we have analyzed IRS2 signaling in white mononuclear blood cells (WMBCs) from MetS patients with and without IR. Additionally, we have studied *apoE-null* mice with an intact *Irs2* gene ($apoE^{-/-}$) or lacking one allele of *Irs2* ($apoE^{-/-}Irs2^{+/-}$ mice), and primary VSMCs and macrophages derived from these animals.

Materials and Methods

Expanded Materials and Methods can be found in supplemental material (available online at http://atvb.ahajournals.org).

Human Subjects

In compliance with institutional guidelines, subjects were informed of the present study and all agreed to participate. The study was carried out in accordance with the Helsinki Declaration, and the Ethical Committee of the University Clinic of Navarra approved the protocol. The study was performed with samples from 55 unrelated individuals referred to our institution for routine medical work-up after 12 hours of overnight fasting. Clinical screenings were based on medical history, physical examination, and routine analytic tests. Subjects were diagnosed with MetS when 3 or more of the AHA/NHLBI criteria for defining this condition were present.[1] The following criteria were adopted. Central obesity: waist circumference ≥102 cm in men and ≥88 cm in women; hypertriglyceridemia: triglycerides ≥1.7 mmol/L or use of medication to reduce triglycerides; low HDL cholesterol: HDL cholesterol <1.03 mmol/L in men and <1.3 mmol/L in women or use of medication to increase HDL cholesterol; high blood pressure: systolic blood pressure (SBP) ≥130 mm Hg, diastolic blood pressure (DBP) ≥85 mm Hg, or use of antihypertensive medication; high fasting glucose: glucose ≥5.55 mmol/L or use of medication to reduce glucose.

IR was diagnosed when the homeostasis model assessment (HOMA) index (fasting glucose [mmol/L]×fasting insulin [μU/mL]/22.5) was equal or greater than the median in normal-weight subjects plus 2.5 standard deviations (HOMA ≥3.3). Using this criterium, we identified 30 patients with IR within the studied population.

Mice and Diets

Care of animals was in accordance with institutional guidelines. $Irs2^{-/-}$ (C57BL/6J)[10] and $apoE^{-/-}$ (C57BL/6J, Charles River Lyon, France) mice were crossbred to generate $apoE^{-/-}Irs2^{+/-}$ mice. Genotyping was done by polymerase chain reaction (PCR) as described.[10,12] After weaning, male mice were maintained on a low-fat (control) standard diet (2.8% fat; Panlab, Barcelona, Spain) or placed on an atherogenic diet (10.8% total fat, 0.75% cholesterol, S8492-E010, Ssniff, Germany) for the indicated periods of time.

Results

Irs2 and *Akt2* Expression Is Decreased in WMBCs and Inversely Correlates With Insulin Levels and HOMA Index in Insulin-Resistant MetS Patients

The demographic and clinical characteristics of the MetS patients included in our studies are summarized in supplemental Table I (available online at http://atvb.ahajournals.org). Patients were classified as insulin-sensitive or insulin-resistant based on the HOMA index (see methods). No significant differences in gender distribution, age, and frequency of cardiovascular medications were observed between both groups. However, insulin-resistant patients presented higher body mass index (BMI), waist circumference, DBP, HOMA index, and plasma levels of insulin, oxidized LDL (oxLDL), and metalloproteinase-9 (MMP-9), and lower plasma HDL-cholesterol levels as compared with insulin-sensitive patients. No significant differences in the remaining parameters were noted between the 2 groups of patients. Thus, IR is associated with higher risk of CVD in our cohort of MetS patients.

Given that total genetic ablation of *Irs2* in fat-fed $apoE^{-/-}$ mice produces IR and accelerates atherosclerosis[12,13] and that IRS proteins signal in part through the PI3K/AKT pathway,[8] we examined *Irs2* and *Akt* expression in WMBCs from both groups of patients. Quantitative real-time PCR (qPCR) analysis revealed reduced *Irs2* and *Akt2* mRNA levels in insulin-resistant versus insulin-sensitive subjects, although only differences in *Akt2* reached statistical significance (Figure 1A).We also found increased expression of *Irs1* in insulin-resistant versus insulin-sensitive individuals ($P=0.029$), whereas *Akt1* and *Akt3* were expressed at similar level in both groups of patients (Figure 1A). Correlation studies demonstrated a significant and positive bivariate correlation between *Irs2* and *Akt2* expression in all the MetS patients ($r^2=0.66$, $P<0.001$, Figure 1B), which remained highly significant after controlling for age and sex ($r^2=0.63$, $P<0.001$), and when analyzing separately insulin-sensitive ($r^2=0.69$, $P<0.001$) and insulin-resistant ($r^2=0.46$, $P<0.001$) patients.

In insulin-resistant patients, mRNA expression levels of *Irs2* and *Akt2* in WMBCs exhibited a statistically significant inverse correlation with plasma insulin levels (Figure 1C and 1E) and the HOMA index (Figure 1D and 1F). These associations were not observed in insulin-sensitive patients (*Irs2* versus insulin: $r^2=0.039$, $P=0.342$; *Irs2* versus HOMA: $r^2=0.051$, $P=0.278$; *Akt2* versus insulin: $r^2=0.02$, $P=0.500$; *Akt2* versus HOMA: $r^2=0.022$, $P=0.484$). Additional association studies are presented in supplemental Tables II through V. These results indicate that hyperinsulinemia and IR in MetS patients are associated with downregulation of *Irs2* and its downstream effector *Akt2* in WMBCs.

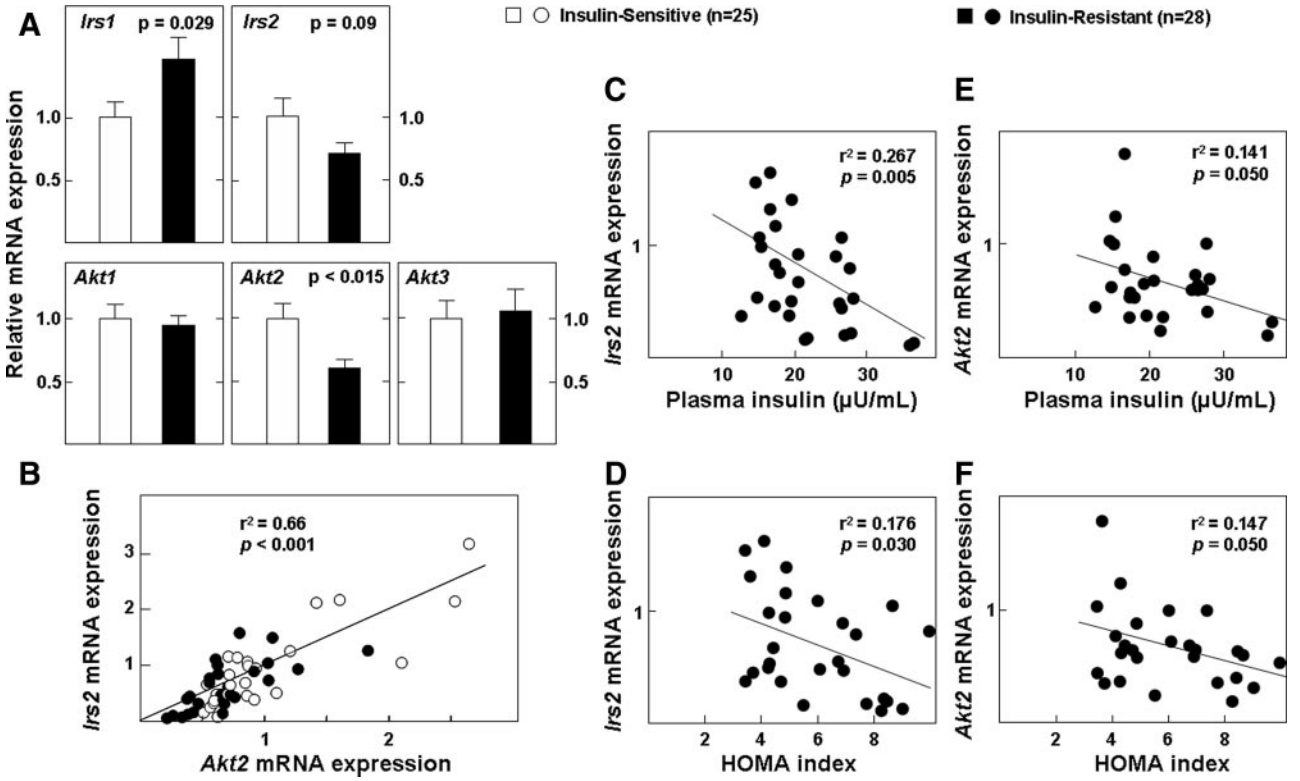

Figure 1. qPCR analysis in WMBCs from MetS patients. A, Insulin-resistant compared to insulin-sensitive patients (=1). B, Correlation between *Irs2* and *Akt2* mRNA for all MetS patients. C through F, Regression analysis of *Irs2* (C and D) and *Akt2* (E and F) mRNA revealed significant associations with plasma insulin (C and E) and HOMA index (D and F) in insulin-resistant patients.

Partial Inactivation of *Irs2* in *ApoE*$^{-/-}$ Mice Combined With Severe Hypercholesterolemia Produces Increased Glucose Intolerance and Mild Hyperinsulinemia and Accelerates Atherosclerosis

We next sought to generate an animal model with moderate reductions in *Irs2* expression to determine whether this alteration observed in insulin-resistant MetS patients accelerates atherosclerosis. To this end, we partially inactivated the *Irs2* gene in *apoE*$^{-/-}$ mice, which spontaneously develop hypercholesterolemia and complex atherosclerotic lesions resembling those observed in humans, which can be accelerated by a high-fat cholesterol-rich diet.[17] Mice received either standard chow or were challenged for 3 months with a high-fat cholesterol-rich atherogenic diet. Under either dietary regimen, partial disruption of *Irs2* did not influence circulating glucose levels (Figure 2A and 2B). Similarly, fasting plasma insulin levels did not differ between *apoE*$^{-/-}$ and *apoE*$^{-/-}$*Irs2*$^{+/-}$ mice fed control diet (Figure 2A). However, on a high-fat diet, a trend toward increased fasting plasma insulin was observed in *apoE*$^{-/-}$*Irs2*$^{+/-}$ mice compared with *apoE*$^{-/-}$ mice (1.00±0.17 versus 0.65±0.14 μg/dL, respectively, $P=0.074$; Figure 2B). Glucose tolerance measured by the area under the curve (AUC) was similar in *apoE*$^{-/-}$*Irs2*$^{+/-}$ and *apoE*$^{-/-}$ mice fed control diet (Figure 2C), whereas, fat-fed *apoE*$^{-/-}$*Irs2*$^{+/-}$ mice were more glucose intolerant than *apoE*$^{-/-}$ counterparts on a high-fat diet ($P<0.05$, Figure 2D). Under both dietary regimens, glucose-stimulated insulin secretion was similar in both groups of mice, as revealed by the AUC (Figure 2C and 2D). Likewise, body weight did not differ statistically between control and fat-fed *apoE*$^{-/-}$*Irs2*$^{+/-}$ and *apoE*$^{-/-}$ mice (data not shown), thus excluding obesity as a principal factor in the aforementioned metabolic differences developed by *apoE*$^{-/-}$*Irs2*$^{+/-}$ mice.

Circulating levels of total cholesterol (Total-C), HDL-C, and triacylglycerides (TAG) were indistinguishable between *apoE*$^{-/-}$ and *apoE*$^{-/-}$*Irs2*$^{+/-}$ mice fed either control (Figure 2E) or atherogenic (Figure 2F) diet. As expected, levels of plasma Total-C and TAG in fat-fed mice were increased in comparison to prediet values. These findings suggest that lipid metabolism in *apoE*$^{-/-}$ mice is unaffected by deletion of one allele of *Irs2*.

As shown in Figure 3A, oil red O staining revealed similar extent of atherosclerosis in the aortic arch of *apoE*$^{-/-}$ and *apoE*$^{-/-}$*Irs2*$^{+/-}$ mice fed control diet (Total-C ≈300 mg/dL, cf. Figure 2E). In contrast, atherosclerosis burden was significantly increased in fat-fed *apoE*$^{-/-}$*Irs2*$^{+/-}$ mice (Total-C>550 mg/dL, cf. Figure 2F, postdiet values) receiving the atherogenic diet for 2 months (aortic root, supplemental Figure IA) and 3 months (aortic arch, Figure 3A). We also found that neointimal accumulation of Mac3-immunoreactive macrophages, SMα -actin-immunoreactive VSMCs, and collagen was undistinguishable when comparing *apoE*$^{-/-}$ and *apoE*$^{-/-}$*Irs2*$^{+/-}$ mice fed either standard chow or atherogenic diet (Figure 3B, and supplemental Figure IB).

We next investigated the consequences of reduced *Irs2* expression on the uptake of modified LDL by macrophages, a key event in atherosclerosis.[18] Macrophages from *apoE*$^{-/-}$

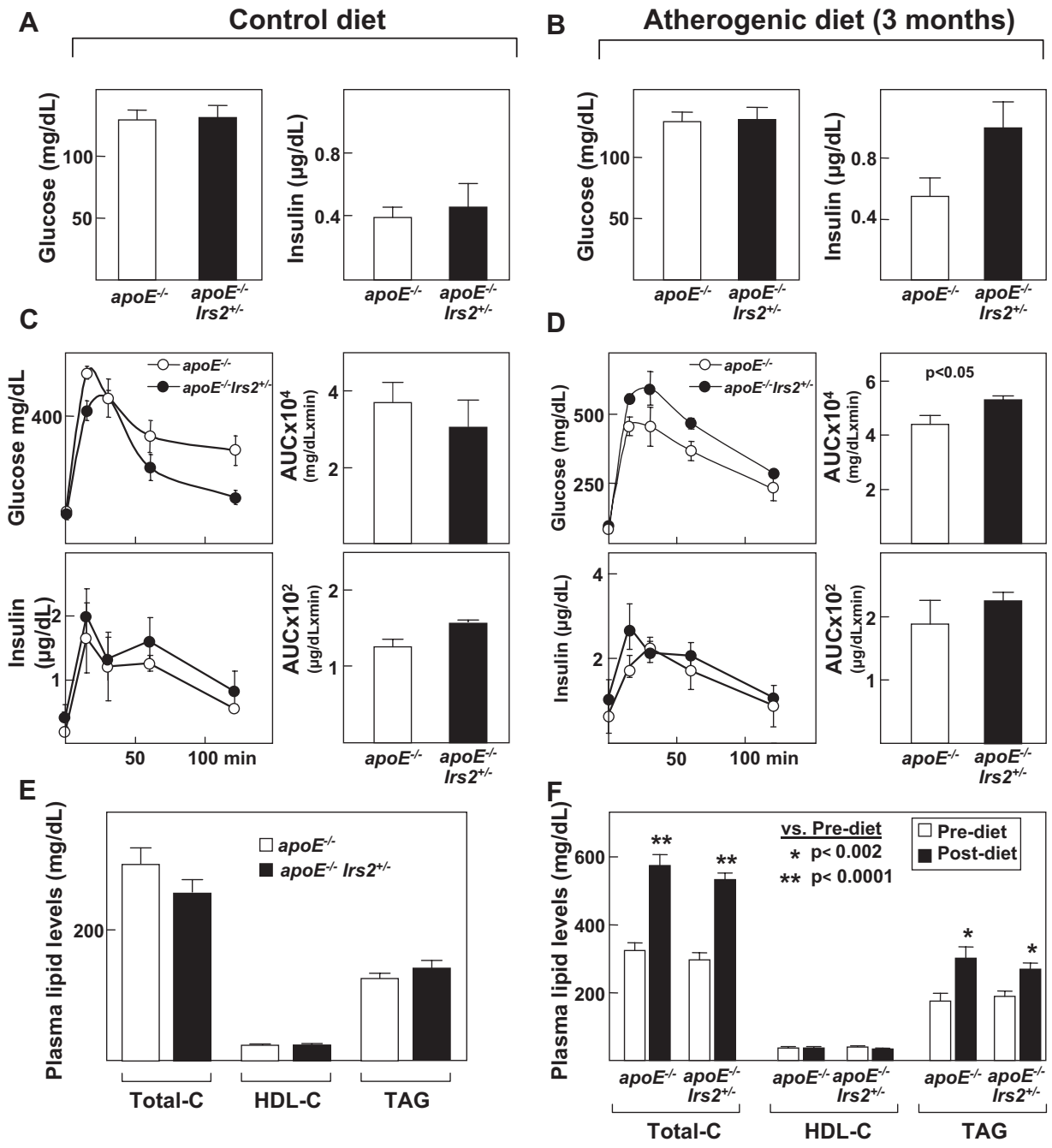

Figure 2. Metabolic characterization of mice. A*apoE*$^{-/-}$ and a*poE*$^{-/-}$*Irs2*$^{+/-}$ mice received either control (A, C, and E) or atherogenic (B, D, and F) diet. A and B, Fasting plasma glucose and insulin. C and D, Glucose tolerance test showing plasma glucose and insulin levels and the corresponding area under the curve (AUC). E and F, Fasting plasma total cholesterol (Total-C), HDL-C, and TAG.

Irs2$^{+/-}$ mice exhibited a 30% increase in AlexaFluor488-acLDL uptake compared to *apoE*$^{-/-}$ controls (Figure 3C), coinciding with higher mRNA levels of CD36 and SRA (Figure 3D), the two main scavenger receptors involved in the uptake of modified LDLs by neointimal macrophages.

Effect of Partial *Irs2* Inactivation on Aortic Expression of Genes Related to Insulin Signaling

To further investigate the underlying mechanisms by which partial inactivation of *Irs2* in *apoE*$^{-/-}$ mice aggravates diet-induced atherosclerosis, we used a pathway-focused RT-PCR array which profiles the expression of 84 genes related to insulin action (supplemental Table VI and expanded Materials and Methods). We analyzed atheroma-rich aortic tissue obtained from mice maintained for 2 months on a high-fat diet. The array analysis revealed changes in the expression of 14 genes in aorta of *apoE*$^{-/-}$*Irs2*$^{+/-}$ versus *apoE*$^{-/-}$ mice (3 with $P=0.06$ and 11 with at least $P<0.05$) (supplemental Figure II). As expected, *Irs2* mRNA expression was significantly reduced in *apoE*$^{-/-}$*Irs2*$^{+/-}$ aorta. Among the altered genes, several are related with glucose and lipid metabolism (*G6pc, G6pc2, LDLr*) whereas others encode kinases and

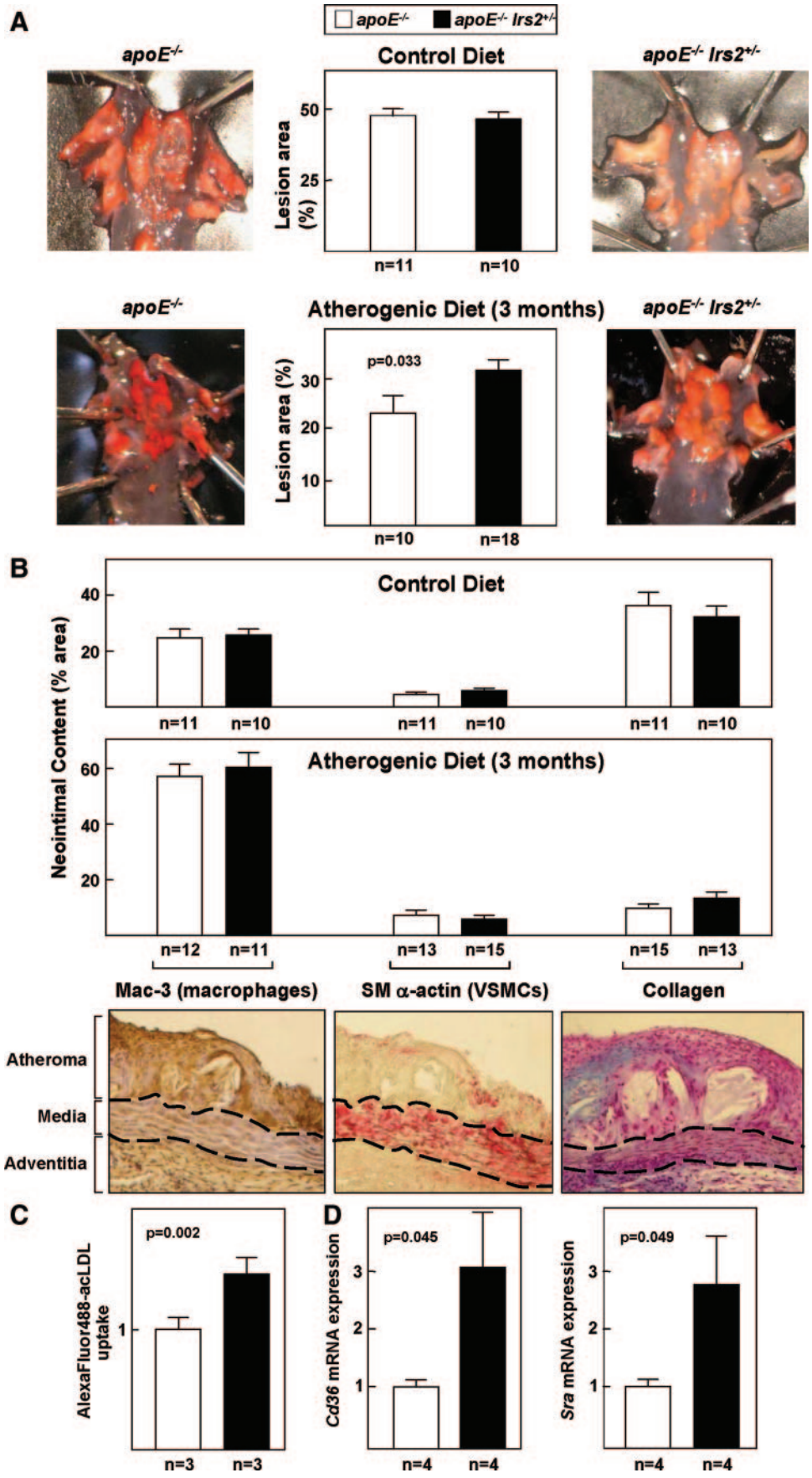

Figure 3. *Irs2* partial disruption increases atherosclerosis and macrophage acLDL uptake and scavenger receptor expression. A, Atherosclerosis burden (oil red O–stained aortic arch). B, Neointimal content of Mac3-immunoreactive and SMα-actin–immunoreactive cells and collagen (representative images from fat-fed *apoE*$^{-/-}$*Irs2*$^{+/-}$). C and D, Macrophage AlexaFluor488-acLDL uptake and qPCR of CD36 and SRA (relative to *apoE*$^{-/-}$).

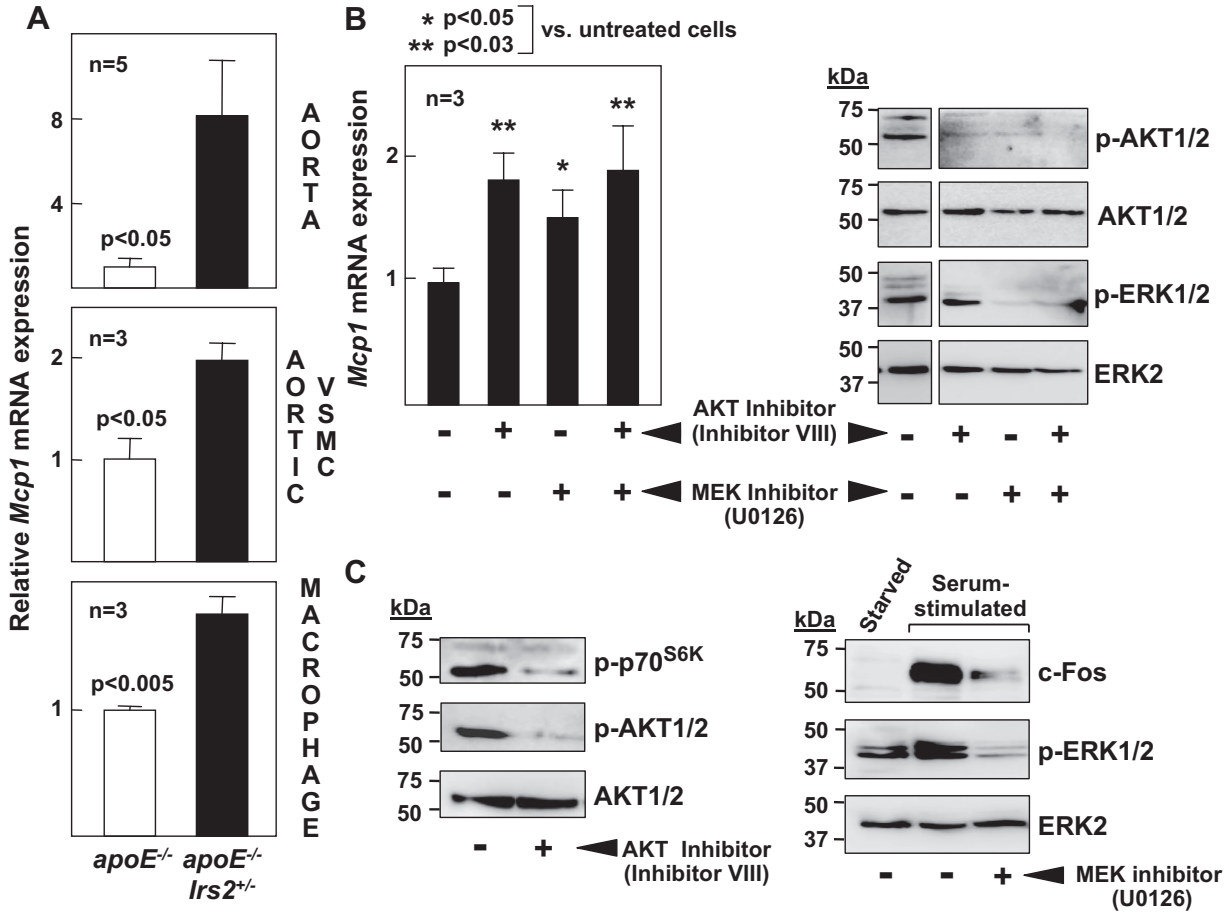

Figure 4. *Mcp1* upregulation by *Irs2* partial inactivation and AKT2 or ERK1/2 pharmacological inhibition. A, qPCR in VSMCs, macrophages, and aorta from fat-fed mice ($apoE^{-/-}$=1). B, Rat VSMCs were subjected to qPCR (Left, untreated cells=1) and Western blot (Right, p-AKT1/2: phosphorylated AKT1/2; p-ERK1/2: phosphorylated ERK1/2). C, Western blots in rat VSMCs.

phosphatases (*Dusp14, Nck1, Prkc*), transcription factors (*Cebpa, Klf10*), and scaffold protein genes (*Shc1*). Interestingly, $apoE^{-/-}Irs2^{+/-}$ aorta exhibited reduced *Akt2, Rras*, and *Hras1* mRNA levels. These results clearly demonstrate that the *Irs2/Akt2/Ras* insulin-signaling effector pathway is downregulated in aortic tissue of fat-fed $apoE^{-/-}Irs2^{+/-}$ mice.

Both Partial *Irs2* Genetic Inactivation and Pharmacological Inhibition of AKT or ERK1/2 Enhance *Mcp1* Expression

Atherosclerosis, T2DM, and IR are characterized by chronic inflammation in different tissues.[3–5,19,20] qPCR revealed increased expression of the proinflammatory cytokine *Mcp1* in atherosclerotic plaque-rich aorta of $apoE^{-/-}Irs2^{+/-}$ mice as well as in primary cultures of VSMCs and macrophages obtained from these animals versus $apoE^{-/-}$ controls (Figure 4A). Given the results of our expression studies in aorta showing reduced mRNA level of *Akt2, Hras 1*, and *Rras* (supplemental Figure II), we sought to assess whether defective signaling through AKT2 or ERK1/2 (a downstream effector of RAS signaling) might be linked to the increased *Mcp1* expression associated with reduced expression of *Irs2*. Indeed, pharmacological inhibition of either AKT (inhibitor VIII) or ERK1/2 (U0126) increased *Mcp1* mRNA expression in cultures of rat VSMCs (Figure 4B). Western blot analysis confirmed the inhibition of AKT and ERK, as indicated by reduced accumulation of phosphorylated (active) AKT1/2 and ERK1/2 (Figure 4B, pAKT1/2, pERK1/2) in treated VSMCs. Moreover, inhibitor VIII and U0126 markedly reduced, respectively, the phosphorylation of $p70^{S6K}$ (which is triggered on AKT activation) and of serum-inducible c-Fos upregulation (which depends on ERK1/2 activation; Figure 4C), thus providing functional validation of the efficacy of these drugs in our experimental settings.

Discussion

Irs2-null mice develop T2DM- and MetS-like alterations (eg, IR, hyperinsulinemia, glucose intolerance, hypertension, moderate hyperlipidemia).[9–11] Recently, we and others reported that total ablation of *Irs2* accelerates atherosclerosis in severely hypercholesterolemic $apoE^{-/-}$ mice.[12,13] Novel findings in the present study include: (1) the demonstration that increased risk of CVD in insulin-resistant versus insulin-sensitive MetS patients is associated with reduced expression of *Irs2* in WMBCs, and that a moderate reduction in *Irs2* expression is sufficient to accelerate atherosclerosis in severely hypercholesterolemic $apoE^{-/-}Irs2^{+/-}$ mice, which display characteristics of MetS and IR; (2) the identification in aorta of changes in the expression of insulin-related genes potentially involved in augmented atherosclerosis in $apoE^{-/-}$

Irs2$^{+/-}$ mice, including the downregulation of Akt2 and Ras; and (3) the identification of defective IRS2/AKT and IRS2/RAS/ERK1/2 signaling as mechanisms of upregulating the expression of proatherogenic MCP1.

Reduced expression of *Ins-r, Irs2*, and *Akt2* has been reported in pancreatic β-cells of T2DM/IR patients.[16] However, our study is the first to analyze the expression of these signaling molecules in WMBCs from insulin-resistant and insulin-sensitive patients (Figure 1A). Notably, in accordance with the notion that AKT acts downstream of IRS2, we found a direct correlation between the level of *Irs2* and *Akt2* mRNA, both when considering all MetS patients (Figure 1B) and when analyzing separately insulin-sensitive and insulin-resistant subjects. We also found that levels of *Irs2* and *Akt2* mRNA were inversely correlated with plasma insulin levels and the HOMA index only in insulin-resistant patients (Figure 1C through 1F). Thus, hyperinsulinemia and IR in humans are associated with the downregulation of *Irs2* and *Akt2* in cell types which play major roles in the pathogenesis of T2DM and atherosclerosis. We also found similar level of *Akt1* and *Akt3* in both groups of MetS patients and higher *Irs1* expression in insulin-resistant subjects, perhaps as a compensatory mechanism, a possibility which deserves further investigation. Additional studies are also warranted to clarify the relative contribution of defined subpopulations of WMBCs in the establishment of the observed differences between insulin-sensitive and insulin-resistant MetS patients.

We and others have previously reported that fat-fed *apoE*$^{-/-}$ mice with complete deficiency for IRS-2 exhibit features of MetS (severe dyslipidemia, hyperinsulinemia, glucose intolerance, IR) and accelerated atherosclerosis.[12,13] To address whether a moderate reduction in *Irs2* expression (comparable to that which we observed in the WMBCs of insulin-resistant patients with MetS) might have pathological consequences in an animal model, we generated a*poE*$^{-/-}$*Irs2*$^{+/-}$ mice which lack only one allele of *Irs2*. In response to high-fat feeding, these mice developed severe hypercholesterolemia (Total-C>550 mg/dL), higher glucose intolerance, and a trend toward hyperinsulinemia as compared to similarly hypercholesterolemic *apoE*$^{-/-}$ controls (Figure 2). This MetS-like phenotype of fat-fed a*poE*$^{-/-}$*Irs2*$^{+/-}$ mice was associated with significantly enhanced aortic atherosclerosis, without changes in plaque composition (eg, macrophage, vascular smooth muscle cell [VSMC], and collagen content; Figure 3, and supplemental Figure I). Notably, none of the differences caused by partial *Irs2* ablation were observed when mice were fed standard chow (Total-C <300 mg/dL), suggesting that reduced *Irs2* expression can accelerate atherosclerosis only when combined with other features of MetS such as severe hypercholesterolemia. Interestingly, IR combined with severe hypercholesterolemia (>700 mg/dL) was also associated with severe atherosclerosis in fat-fed liver *Ins-r*–deficient mice.[21] We also noted higher expression of the scavenger receptors SRA and CD36 and increased uptake of acLDL in a*poE*$^{-/-}$*Irs2*$^{+/-}$ versus apoE$^{-/-}$ macrophages (Figure 3C and 3D). Similar findings have been previously reported for *Ins-r*–deficient and ob/ob mouse macrophages.[15,22] Thus, increased macrophage uptake of modified LDLs through upregulation of SRA and CD36 appears to contribute to accelerated atherosclerosis in different MetS murine models.

As fat-fed *apoE*$^{-/-}$*Irs2*$^{+/-}$ mice seemed an appropriate model to investigate how impaired insulin-dependent signaling promotes atherosclerosis, we used aorta from these mice to investigate the consequences of reduced *Irs2* on the expression of 84 genes implicated in insulin-signaling using a qPCR array (supplemental Table VI and supplemental Figure II). As expected, our gene profiling study confirmed a significant reduction in *Irs2* mRNA in atheroma-rich aorta from fat-fed *apoE*$^{-/-}$*Irs2*$^{+/-}$ versus apoE$^{-/-}$ mice. The expression of *Akt2* and *Ras* was also significantly diminished in aorta of fat-fed *apoE*$^{-/-}$*Irs2*$^{+/-}$ mice, indicating a correlation between a moderate reduction of *Irs2* expression and the downregulation of 2 major pathways which mediate insulin signaling. Remarkably, insulin-dependent IRS2/PI3K/AKT and IRS1/ERK1/2 signaling are impaired in macrophages from db/db and ob/ob diabetic mice,[22,23] and in human adipocytes from T2DM patients,[24] respectively. It is also noteworthy that *Akt2* ablation in the mouse causes major alterations in glucose homeostasis and insulin sensitivity, leading to IR and T2DM.[25,26] Therefore, our results extend these findings to the cardiovascular system by suggesting a mechanistic link between impaired AKT2- and RAS-dependent signaling in aortic tissue and accelerated atherosclerosis in fat-fed *apoE*$^{-/-}$*Irs2*$^{+/-}$ mice.

The proatherogenic role of MCP1 has been firmly established.[27,28] Thus, the upregulation of *Mcp1* mRNA observed in aorta of fat-fed a*poE*$^{-/-}$*Irs2*$^{+/-}$ mice (Figure 4A) may accelerate atherosclerosis in this model. *Mcp1* expression was also higher in primary VSMCs and macrophages from a*poE*$^{-/-}$*Irs2*$^{+/-}$ mice (Figure 4A). Moreover, this cytokine is upregulated in adipocytes exhibiting IR (IR-3T3-L1 and ob/ob adipocytes)[29] and in platelets from diabetic patients.[30] Our finding that pharmacological inhibition of AKT2 or ERK1/2 upregulates *Mcp1* mRNA in rat VSMCs (Figure 4B) is consistent with the notion that accelerated atherosclerosis in MetS conditions is attributable, at least in part, to defective IRS2-AKT2 and IRS2-RAS/ERK1/2 pathways and the resulting upregulation of *Mcp1* in various cell types involved in atherothrombosis (eg, VSMCs, macrophages, platelets, adipocytes). However, additional studies are needed to firmly establish causal relationships between human MetS states, *Mcp1* upregulation, and dysfunctional IRS2-AKT2- and IRS2-RAS/ERK1/2–dependent signaling.

In summary, our studies demonstrate that WMBCs from MetS patients with IR display diminished expression of *Irs2* and its downstream effector *Akt2* compared to insulin-sensitive MetS patients, suggesting a mechanistic link between reduced IRS2 expression and human metabolic diseases. Indeed, the moderate reduction of *Irs2* expression achieved in fat-fed *apoE*$^{-/-}$*Irs2*$^{+/-}$ mice is sufficient to produce MetS-like symptoms and accelerate atherosclerosis. Our studies with aortic tissue, primary VSMCs, and macrophages demonstrate that partial *Irs2* inactivation impairs AKT2- and Ras/ERK1/2-dependent signaling, leading to augmented MCP1 expression and enhanced CD36 and SRA scavenger receptor expression and macrophage acLDL uptake beyond hypercholesterolemia. These findings highlight

defective IRS2-associated AKT2- and Ras/ERK1/2-dependent signaling as a potential mechanism underlying accelerated atherosclerosis in MetS/IR states.

Acknowledgments

We thank Núria Ruiz for help with statistical analysis and M. J. Andrés-Manzano for help preparing figures.

Sources of Funding

This work was supported by grants from the Spanish Ministry of Education and Science and the European Regional Development Fund (SAF2004-03057, SAF2007-62110, SAF2007-62533), Instituto de Salud Carlos III (RECAVA, grants RD06/0014/0008, RD06/0014/0021, CIBERDEM), Generalitat Valenciana (GV/2007/164), Sociedad Española de Cardiología (Beca Novartis 2006), European Union (InGenious HyperCare, grant LSHM-CT-2006-037093), and from the agreement between the Foundation for Applied Medical Research (FIMA) and "UTE project CIMA". H.G.-N. received salary support from the European Union (Marie Curie fellowship MEIF-CT-2005-024393). M.V.-C. was a fellow from the Regional Government of Valencia and from Instituto Danone.

Disclosures

None.

References

1. Grundy SM, Cleeman JI, Daniels SR, Donato KA, Eckel RH, Franklin BA, Gordon DJ, Krauss RM, Savage PJ, Smith SC Jr, Spertus JA, Costa F. Diagnosis and management of the metabolic syndrome: an American Heart Association/National Heart, Lung, and Blood Institute Scientific Statement. *Circulation*. 2005;112:2735–2752.
2. Beckman JA, Creager MA, Libby P. Diabetes and atherosclerosis: epidemiology, pathophysiology, and management. *JAMA*. 2002;287:2570–2581.
3. Kuiper J, van Puijvelde GH, van Wanrooij EJ, van Es T, Habets K, Hauer AD, van den Berkel TJ. Immunomodulation of the inflammatory response in atherosclerosis. *Curr Opin Lipidol*. 2007;18:521–526.
4. Mallat Z, Tedgui A. Cytokines as regulators of atherosclerosis in murine models. *Current Drug Targets*. 2007;8:1264–1272.
5. Rader DJ, Daugherty A. Translating molecular discoveries into new therapies for atherosclerosis. *Nature*. 2008;451:904–913.
6. Semenkovich CF. Insulin resistance and atherosclerosis. *J Clin Invest*. 2006;116:1813–1822.
7. Kanter JE, Johansson F, LeBoeuf RC, Bornfeldt KE. Do glucose and lipids exert independent effects on atherosclerotic lesion initiation or progression to advanced plaques? *Circ Res*. 2007;100:769–781.
8. Nandi A, Kitamura Y, Kahn CR, Accili D. Mouse models of insulin resistance. *Physiol Rev*. 2004;84:623–647.
9. Burks DJ, de Mora JF, Schubert M, Withers DJ, Myers MG, Towery HH, Altamuro SL, Flint CL, White MF. IRS-2 pathways integrate female reproduction and energy homeostasis. *Nature*. 2000;407:377–382.
10. Withers DJ, Gutierrez JS, Towery H, Burks DJ, Ren JM, Previs S, Zhang Y, Bernal D, Pons S, Shulman GI, Bonner-Weir S, White MF. Disruption of IRS-2 causes type 2 diabetes in mice. *Nature*. 1998;391:900–904.
11. Kubota N, Tobe K, Terauchi Y, Eto K, Yamauchi T, Suzuki R, Tsubamoto Y, Komeda K, Nakano R, Miki H, Satoh S, Sekihara H, Sciacchitano S, Lesniak M, Aizawa S, Nagai R, Kimura S, Akanuma Y, Taylor SI, Kadowaki T. Disruption of insulin receptor substrate 2 causes type 2 diabetes because of liver insulin resistance and lack of compensatory beta-cell hyperplasia. *Diabetes*. 2000;49:1880–1889.
12. Gonzalez-Navarro H, Vila-Caballer M, Pastor MF, Vinue A, White MF, Burks D, Andres V. Plasma insulin levels predict the development of atherosclerosis when IRS2 deficiency is combined with severe hypercholesterolemia in apolipoprotein E-null mice. *Front Biosci*. 2007;12:2291–2298.
13. Baumgartl J, Baudler S, Scherner M, Babaev V, Makowski L, Suttles J, McDuffie M, Fazio S, Kahn CR, Hotamisligil GS, Krone W, Linton M, Bruning JC. Myeloid lineage cell-restricted insulin resistance protects apolipoproteinE-deficient mice against atherosclerosis. *Cell Metab*. 2006;3:247–256.
14. Gruen ML, Saraswathi V, Nuotio-Antar AM, Plummer MR, Coenen KR, Hasty AH. Plasma insulin levels predict atherosclerotic lesion burden in obese hyperlipidemic mice. *Atherosclerosis*. 2006;186:54–64.
15. Han S, Liang CP, Devries-Seimon T, Ranalletta M, Welch CL, Collins-Fletcher K, Accili D, Tabas I, Tall AR. Macrophage insulin receptor deficiency increases ER stress-induced apoptosis and necrotic core formation in advanced atherosclerotic lesions. *Cell Metab*. 2006;3:257–266.
16. Gunton JE, Kulkarni RN, Yim S, Okada T, Hawthorne WJ, Tseng YH, Roberson RS, Ricordi C, O'Connell PJ, Gonzalez FJ, Kahn CR. Loss of ARNT/HIF1beta mediates altered gene expression and pancreatic-islet dysfunction in human type 2 diabetes. *Cell*. 2005;122:337–349.
17. Meir KS, Leitersdorf E. Atherosclerosis in the apolipoprotein E-deficient mouse: a decade of progress. *Arterioscler Thromb Vasc Biol*. 2004;24:1006–1014.
18. Glass CK, Witztum JL. Atherosclerosis. the road ahead. *Cell*. 2001;104:503–516.
19. Lumeng CN, Bodzin JL, Saltiel AR. Obesity induces a phenotypic switch in adipose tissue macrophage polarization. *J Clin Invest*. 2007;117:175–184.
20. Furuhashi M, Tuncman G, Gorgun CZ, Makowski L, Atsumi G, Vaillancourt E, Kono K, Babaev VR, Fazio S, Linton MF, Sulsky R, Robl JA, Parker RA, Hotamisligil GS. Treatment of diabetes and atherosclerosis by inhibiting fatty-acid-binding protein aP2. *Nature*. 2007;447:959–965.
21. Biddinger SB, Hernandez-Ono A, Rask-Madsen C, Haas JT, Aleman JO, Suzuki R, Scapa EF, Agarwal C, Carey MC, Stephanopoulos G, Cohen DE, King GL, Ginsberg HN, Kahn CR. Hepatic insulin resistance is sufficient to produce dyslipidemia and susceptibility to atherosclerosis. *Cell Metab*. 2008;7:125–134.
22. Liang CP, Han S, Senokuchi T, Tall AR. The macrophage at the crossroads of insulin resistance and atherosclerosis. *Circ Res*. 2007;100:1546–1555.
23. Hartman ME, O'Connor JC, Godbout JP, Minor KD, Mazzocco VR, Freund GG. Insulin receptor substrate-2-dependent interleukin-4 signaling in macrophages is impaired in two models of type 2 diabetes mellitus. *J Biol Chem*. 2004;279:28045–28050.
24. Ost A, Danielsson A, Liden M, Eriksson U, Nystrom FH, Stralfors P. Retinol-binding protein-4 attenuates insulin-induced phosphorylation of IRS1 and ERK1/2 in primary human adipocytes. *Faseb J*. 2007;21:3696–3704.
25. Cho H, Mu J, Kim JK, Thorvaldsen JL, Chu Q, Crenshaw EB III, Kaestner KH, Bartolomei MS, Shulman GI, Birnbaum MJ. Insulin resistance and a diabetes mellitus-like syndrome in mice lacking the protein kinase Akt2 (PKB beta). *Science*. 2001;292:1728–1731.
26. Garofalo RS, Orena SJ, Rafidi K, Torchia AJ, Stock JL, Hildebrandt AL, Coskran T, Black SC, Brees DJ, Wicks JR, McNeish JD, Coleman KG. Severe diabetes, age-dependent loss of adipose tissue, and mild growth deficiency in mice lacking Akt2/PKB beta. *J Clin Invest*. 2003;112:197–208.
27. Peters W, Charo IF. Involvement of chemokine receptor 2 and its ligand, monocyte chemoattractant protein-1, in the development of atherosclerosis: lessons from knockout mice. *Curr Opin Lipidol*. 2001;12:175–180.
28. Bursill CA, Channon KM, Greaves DR. The role of chemokines in atherosclerosis: recent evidence from experimental models and population genetics. *Curr Opin Lipidol*. 2004;15:145–149.
29. Sartipy P, Loskutoff DJ. Monocyte chemoattractant protein 1 in obesity and insulin resistance. *Proc Natl Acad Sci U S A*. 2003;100:7265–7270.
30. Nomura S, Shouzu A, Omoto S, Nishikawa M, Fukuhara S. Significance of chemokines and activated platelets in patients with diabetes. *Clin Exper Immunol*. 2000;121:437–443.

Supplementary Material

Molecular mechanisms of atherosclerosis in metabolic syndrome: Role of reduced IRS2-dependent signaling

Herminia González-Navarro, Ángela Vinué, Marian Vila-Caballer, Ana Fortuño, Oscar Beloqui, Guillermo Zalba, Deborah Burks, Javier Díez, Vicente Andrés

Expanded figure legends

Fig.1. mRNA levels of *Irs2* and *Akt2* in WMBCs are decreased in insulin-resistant MetS patients and inversely correlate with plasma insulin levels and HOMA index. **(A)** qPCR analysis of *Irs1, Irs2*, *Akt1, Akt2* and *Akt3* in WMBCs. Insulin-resistant patients are compared to insulin-sensitive patients (=1). Results were normalized by endogenous *Gapdh* expression, which was undistinguishable in both groups ($p>0.05$). **(B)** Correlation between *Irs2* and *Akt2* mRNA expression levels for all MetS patients. Regression analysis of *Irs2* **(C,D)** and *Akt2* **(E,F)** mRNA levels determined by qPCR revealed significant associations with plasma insulin levels **(C,E)** and HOMA index **(D,F)** in insulin-resistant MetS patients.

Fig.2. Metabolic characterization of *apoE*$^{-/-}$*Irs2*$^{+/-}$ and *apoE*$^{-/-}$ mice. Plasma glucose and insulin levels in mice fed control diet **(A)** or challenged with atherogenic diet for 3 months **(B)** (*apoE*$^{-/-}$*Irs2*$^{+/-}$: n=10 and n=16, respectively; *apoE*$^{-/-}$: n=13 and n=10, respectively) after overnight fasting. Glucose tolerance test in mice fed control diet **(C)** or atherogenic diet for 3 months **(D),** showing plasma glucose and insulin levels and the corresponding AUC (n=6). **(E)** Fasting plasma total cholesterol (Total-C), HDL cholesterol (HDL-C) and TAG of 10-month-old *apoE*$^{-/-}$*Irs2*$^{+/-}$ (n=11) and *apoE*$^{-/-}$ (n=10)

mice on control diet. **(F)** The same parameters were measured in mice before and after 3 months of atherogenic diet (n=16 and n=18, respectively).

Fig.3. Partial disruption of *Irs2* increased atherosclerosis and macrophage acLDL uptake and scavenger receptor expression. (A) Quantification of aortic arch atherosclerosis expressed as percentage of lesional area (stained by Oil Red O) for mice fed control diet for 10 months or atherogenic diet for 3 months. **(B)** Neointimal content (%) of Mac3-immunoreactive macrophages, SMα-actin-immunoreactive VSMCs and collagen in mice fed control diet for 10 months or atherogenic diet for 3 months. The photomicrograps show representative images (from fat-fed a*poE*$^{-/-}$*Irs2*$^{+/-}$mice). The discontinuous lines mark the approximate contour of the tunica media. **(C)** AlexaFluor488-acLDL uptake is increased in *apoE*$^{-/-}$*Irs2*$^{+/-}$ macrophages. Results show the average of three independent experiments and are represented relative to *apoE*$^{-/-}$ (=1). **(D)** qPCR of CD36 and SRA in mouse macrophages (n=4).

Fig.4. Partial inactivation of *Irs2* and pharmacological inhibition of AKT2 or ERK1/2 increases *Mcp1* expression. (A) qPCR of *Mcp1* in VSMCs (n= 3), macrophages (n= 3), and aortic tissue (n=5 pools of 2 vessels per genotype) obtained from fat-fed mice. Results were normalized with *cyclophilin* and were expressed relative to *apoE*$^{-/-}$ (=1). **(B)** Rat VSMCs were treated as indicated. *Left:* qPCR of *Mcp1* (n=3). Results were normalized with *Gapdh* and expressed relative to untreated cells (=1, first bar). *Right:* Western blot analysis of the indicated proteins (p-AKT1/2: phosphorylated AKT1/2; p-ERK1/2: phosphorylated ERK1/2). *p<0.05; **p<0.03 vs. untreated cells. **(C)** Western blot analysis of downstream effectors of AKT (phospho-p70^{S6K}) and ERK (c-Fos) in rat VSMCs treated as indicated.

Expanded Materials and Methods

Metabolic measurements in mice

Circulating glucose and lipid levels in plasma of mice fasted overnight were measured using enzymatic procedures (WAKO, St. Louis, USA) and Glucometer Ascensia Elite (Bayer HealthCare). Insulin levels were determined by ELISA (Mercodia, Sweeden). HDL-cholesterol (HDL-C) was determined after precipitation of the apoB-containing lipoproteins with dextran-sulphate/$MgCl_2$ (SIGMA, St. Louis, USA) as reported.[1] For glucose tolerance test (GTT), mice were injected with glucose (intraperitoneally, 2g/Kg of body weight) and plasma and insulin glucose levels were analyzed at different time-points.

Quantification of atherosclerosis burden

For mice fed standard chow or atherogenic diet for 3 months, the extent of atherosclerosis was determined by Oil Red O staining (80% methanol, 0.2% Oil Red O, SIGMA) of whole mounted aortic arch fixed with 4% paraformaldehyde/PBS as previously described.[1] In mice fed atherogenic diet for 2 months, the aortic arch was snap-frozen for qPCR studies (see below) and lesion size was quantified as the intima-to-media ratio in cross-sections of paraffin-embedded aortic root. A researcher blinded to genotype quantified the extent of atherosclerosis by computer-assisted morphometric analysis (SigmaScan, Pro5).

Immunohistochemical analysis of atheromas

Immunohistopathological examination of atheromas performed by a researcher blinded to genotype included the quantification of the content of macrophages, vascular smooth muscle cells (VSMCs), and collagen (Masson's trichrome stain). VSMCs were identified with mouse anti-SMα-actin monoclonal alkaline phosphatase-conjugated antibody (1/20 dilution, clone 1A4, a-5691, Sigma) and Fast Red substrate (Sigma). Macrophages were detected with a rat anti-Mac3 monoclonal antibody (1/200 dilution, clone M3/84, sc-19991, Santa Cruz Biotechnology), followed by biotin-conjugated goat anti-rat secondary antibody (1/300 dilution, sc-2041, Santa Cruz Biotechnology), HRP-

Streptavidin (STAR5B, AbD SEROTEC) and DAB substrate (BUF021A, AbD SEROTEC). Slides were counterstained with hematoxylin. Images were captured with an Olympus CAMEDIA-C5060 wide zoom digital camera mounted on a stereomicroscope Axiolab, Zeiss).

Primary cell culture

Cultures were maintained at 37 °C in a humidified 5% CO_2 atmosphere. Bone marrow-derived macrophages were obtained from femoral bone marrow suspensions plated at $3x10^6$ cells/mL and differentiated for 7 days in the presence of DMEM/10%FBS/10% macrophage-colony stimulating factor[2]. Mouse and rat aortic VSMC cultures were obtained from thoracic aortas harvested from 3-5 month old animals after two digestions in HBSS/Fungizone medium as described elsewhere.[2] Briefly, the first digestion consisted of type II collagenase (175U/mL, Worthington Biochemical Corp.) incubation to eliminate the adventitia. A second digestion with type II collagenase (175 mg/mL) (Worthington) and type I Elastase (0.5 mg/mL) (Sigma) gave rise to cell suspensions. VSMCs were cultured in 20% FBS/DMEM/Fungizone and used until passage 10. The purity of VSMCs was confirmed with anti-SMα-actin monoclonal alkaline phosphatase-conjugated antibody (1/20 dilution, clone 1A4, a-5691, Sigma) and Fast Red substrate (Sigma).

Western blot analysis and pharmacological inhibition of kinases

Protein extracts were obtained from VSMC cultures (typically 10 cm diameter plates) using ice-cold 50mM Tris-HCl buffer (pH 7.5) containing 1% Triton X-100, 150mM NaCl, 1mM DTT and protease inhibitor Complete Mini cocktail (ROCHE, Mannheim, Germany). Polyacrilamide Gel Electrophoresis and Western blot analysis were done as reported [2] using the following primary antibodies: anti-ERK2 (1/500, sc-154), anti-phospho-ERK1/2 (1/300, sc-7383), anti-c-Fos (1/300, sc-52), anti-Akt1/2 (1/1000, sc-1619) from Santa Cruz Biotechnology, and anti-phospho-Akt1/2 (Ser473) (1/250, 9271) and anti-phosphop70^{S6K} (Ser371) (1/1000, 9208) from Cell Signaling Technology. HRP conjugated secondary antibodies (1/300, Santa Cruz Biotechnology) used were: goat anti-mouse IgG-HRP (sc-2005), goat anti-rabbit IgG-HRP (sc-2004) and donkey anti-

goat IgG-HRP (sc-2056). Immunocomplexes were detected with ECL detection kit (Amersham Biosciences, Piscataway, USA).

For inhibition studies, rat aortic VSMCs were incubated overnight with the MEK inhibitor U0126 (10 μM, Promega) or the AKT Inhibitor VIII (1 μM, Calbiochem). Effective inhibition was first confirmed by Western blot analysis of the phosphorylated (active) forms of AKT (p-AKT) and ERK1/2 (p-ERK1/2). Inhibition was also validated by Western blot of c-Fos and phosphorylated $p70^{S6K}$ ($p\text{-}p70^{S6K}$) as downstream targets of ERK1/2 and AKT, respectively. For c-Fos expression, cells were starved for 48h, pre-incubated 1h with or without the MEK inhibitor U0126 and then serum-stimulated for 2h.

Uptake of acetyladed-low-density lipoproteins (Ac-LDL)

Bone marrow-macrophages from *apoE*$^{-/-}$ (n=3) and *apoE*$^{-/-}$*Irs2*$^{+/-}$ (n=3) mice were incubated for 4 hours with AlexaFluor488-acLDL (1 μg/mL, Invitrogen) in Serum-Free media. After incubation, cells were recovered in complete medium and AlexaFluor488-acLDL uptake was quantified as the median fluorescence intensity (arbitrary units) using a FACsCanto cytometer (BD Bioscience).

Gene expression analysis by quantitative real-time PCR (qPCR)

The TRIzol Reagent (Invitrogen) was used for extracting RNA from aortic tissue of mice fed atherogenic diet for 2 months, from mouse cells and from human white mononuclear blood cells (WMBCs) isolated from peripheral blood samples with Lymphoprep as previously described.[3] RNA purity and concentration was determined by the $A_{260/280}$ ratio.

The studies of Fig.3D and 4A were carried out with RNA (0.5-1μg) retro-transcribed with Superscript III First Strand Synthesis Supermix and Platinum Quantitative PCR Supermix-UDG with Rox dye (both from Invitrogen). Reactions were run on a thermal Cycler 7500 Fast System and results were analyzed with the software provided by the manufacturer (Applied Biosystems). The following primers (Forward: Fw; Reverse: Rv) were designed using the Primer Express programme (Applied Biosystems):

Mouse *Cd36*:

Fw 5'-TCGGAACTGTGGGCTCATTG-3'

Rv 5'-CCTCGGGGTCCTGAGTTATATTTTC-3'

Mouse *Sra*:

Fw 5'-CATGAACGAGAGGATGCTGACT-3

Rv 5'-GGAAGGGATGCTGTCATTGAA-3'

Mouse *Mcp1*:

Fw 5'-GCCCAGCACCAGCACCAG-3'

Rv 5'-GGCATCACAGTCCGAGTC-3'

Mouse *cyclophilin*:

Fw 5'-TGGAGAGCACCAAGACAGACA-3'

Rv 5'-TGCCGGAGTCGACAATGAT-3'

Rat *Mcp1*:

Fw 5'-GCTGCTACTCATTCACTGGCAA-3'

Rv 5'-TGCTGCTGGTGATTCTCTTGTA-3'

Rat *Gapdh*:

Fw 5'-TGCACCACCAACTGCTTA-3'

Rv 5'-GGATGCAGGGATGATGTTC-3'

Human *Irs1*:

Fw-5'-CGGAGAGCGATGGCTTCTC-3'

Rv 5'-GTTTGTGCATGCTCTTGGGTTT-3'

Human *Irs2*:

Fw-5'-CCGACGCCAAGCACAAGTA-3'

Rv 5'-CGGCCACGGCGAAGTA-3'

Human *Akt1*:

Fw 5'-CCGACGCCAAGCACAAGTA-3'

Rv 5'-CGGCCACGGCGAAGTA-3'

Human *Akt2*:

Fw 5'-CAAGGATGAAGTCGCTCACACA-3'

Rv 5'-GAACGGGTGCCTGGTGTTC-3'

Human *Akt3*:

Fw 5'-CCTTGAAATATTCCTTCCAGACAAA-3'

Rv 5'-ACAGCTCGCCCCCATTAAC-3'

Human *Gapdh*:

Fw 5'-ACCACAGTCCATGCCATCAC-3'

Rv 5'-TCCACCACCCTGTTGCTGTA-3'

The studies of Fig. II were done using the Mouse Insulin Signaling Pathway *RT*^{2} *Profiler PCR Array System*, which allows the analysis of 84 genes related to the insulin-signaling pathway and housekeeping genes for normalization (Superarray Bioscience Cat. # PAMM-030, see Table VI and http://www.superarray.com/rt_pcr_product/HTML/PAMM-030A.html). For each array, RNA was extracted with TRIzol Reagent from a pool of 2 aortic archs and cDNA was synthesized using the Reaction-Ready First Strand cDNA synthesis kit (SuperArray Bioscience). For each genotype, 5 independent qPCR arrays were run using the 7500 Fast System Light Cycler and analysis was performed according to the manufacturer's recommendations (Applied Biosystems). Expression in *apoE*$^{-/-}$*Irs2*$^{+/-}$ mice was expressed relative to that in *apoE*$^{-/-}$ mice (=1).

Statistical analysis

Data are presented as mean±SEM. Differences among mouse groups were evaluated by one-way ANOVA with Fisher's post-hoc test (Statview, SAS institute, Cary, USA). Differences in the demographic and clinical characteristics between insulin-resistant and insulin-sensitive patients were assessed by Student's t or Mann-Whitney´s U test. The χ^2 analysis was used to analyze differences among qualitative variables. The Pearson test was used to assess associations between continuous variables in human studies. Multivariate linear regression analysis was performed to evaluate factors related to *Irs2* and *Akt2* human expression. The area under the curve (AUC) was calculated with the *R*-Project programme. Statistical significance was taken at $p \leq 0.05$.

Results

Analysis of all metabolic syndrome (MetS) patients (insulin-sensitive + insulin-resistant) revealed a significant and inverse correlations of WMBC *Irs2* mRNA levels with plasma insulin levels (r^2=0.087, *p*=0.031) and HOMA index (r^2=0.074, *p*=0.050). These associations remained statistically significant in a multivariate analysis after adjusting for age, diastolic blood pressure (DBP), body mass index (BMI), and HDL-cholesterol (Table II and III). Similarly, *Akt2* mRNA levels in WMBC were negatively associated with plasma insulin levels (r^2=0.110, *p*=0.016) and HOMA index (r^2=0.113, *p*=0.050) when analyzing all MetS patients, and these associations remained statistically significant in a multivariate analysis after adjusting for age, DBP, BMI, and HDL-cholesterol (Table IV and V).

References

1. Gonzalez-Navarro H, Vila-Caballer M, Pastor MF, Vinue A, White MF, Burks D, Andres V. Plasma insulin levels predict the development of atherosclerosis when IRS2 deficiency is combined with severe hypercholesterolemia in apolipoprotein E-null mice. *Front Biosci.* 2007;12:2291-2298.
2. Sanz-Gonzalez SM, Barquin L, Garcia-Cao I, Roque M, Gonzalez JM, Fuster JJ, Castells MT, Flores JM, Serrano M, Andres V. Increased p53 gene dosage reduces neointimal thickening induced by mechanical injury but has no effect on native atherosclerosis. *Cardiovasc Res.* 2007;75(4):803-812.
3. Fortuño A, Olivan S, Beloqui O, San Jose G, Moreno MU, Diez J, Zalba G. Association of increased phagocytic NADPH oxidase-dependent superoxide production with diminished nitric oxide generation in essential hypertension. *J Hypertens.* 2004;22(11):2169-2175.

Table I: Demographic and clinical characteristics of MetS patients

	Insulin-sensitive	**Insulin-resistant**	***p value***
Gender (male/female)	22/3	26/4	0.797
Age (years)	55±2	52±2	0.154
BMI (kg/m^2)	28.4±1.2	32.3±0.9	0.012
Waist circumference (cm)	98±2	106±2	0.021
SBP (mm Hg)	137±3	140±3	0.593
DBP (mm Hg)	80±2	88±2	0.032
Glucose (mmol/L)	101±2	106±3	0.152
Insulin (pmol/L)	59.4±4.8	123.6±7.2	<0.001
HOMA index	2.3±0.2	5.4±0.4	<0.001
Total Cholesterol (mg/dL)	216±13	226±11	0.945
LDL-cholesterol (mg/dL)	146±13	150±9	0.938
HDL-cholesterol (mg/dL)	41±2	36±1	0.037
Triglycerides (mg/dL)	153±16	154±12	0.983
von Willebrand Factor (%)	115±13	116±7	0.924
Fibrinogen (mg/dL)	287±12	288±13	0.984
C-reactive protein (mg/dL)	0.31±0.04	0.27±0.03	0.339
Oxidized LDL (U/L)	69±4	86±5	0.017
MMP-9 (ng/mL)	9.9±1.2	14.0±1.4	0.038
Obesity (%)	48	77	0.028
Diabetes (%)	12	17	0.625
Dyslipidemia (%)	84	97	0104
Hypertension (%)	72	77	0.692
Medication			
Antihypertensives (%)	40	47	0.713
Statins (%)	8	7	1.000
Oral hypoglycemics (%)	12	7	0.543

Table II: Association WMBC *Irs2* expression/plasma insulin in multiple linear regression analysis

	β	p *	Partial r^2 (%)
Plasma insulin levels (pmol/L)	-0.25	0.041	8.7
BMI (kg/m^2)	0.004	0.861	0.1
HDL-cholesterol (mg/dL)	-0.11	0.165	2.6
DBP (mm Hg)	-0.003	0.749	0.2
Age (years)	0.13	0.144	3.9

r^2 for the total population was 15.5%

Table III: Association WMBC *Irs2* expression/HOMA index in multiple linear regression analysis

	β	p *	Partial r^2 (%)
HOMA index	-0.084	0.045	7.4
BMI (kg/m^2)	0.003	0.872	0.2
HDL-cholesterol (mg/dL)	-0.11	0.189	1.8
DBP (mm Hg)	-0.002	0.813	0.1
Age (years)	0.16	0.079	5.9

r^2 for the total population was 15.4%

Table IV: Association WMBC *Akt2* expression/plasma insulin in multiple linear regression analysis

	β	p *	Partial r^2 (%)
Plasma insulin levels, pmol/L	-0.023	0.018	11.0
BMI (kg/m^2)	0.022	0.180	2.0
HDL-cholesterol (mg/dL)	-0.0011	0.825	0.1
DBP (mm Hg)	-0.006	0.410	1.1
Age (years)	0.013	0.078	5.7

r^2 for the total population was 19.9%

Table V: Association WMBC *Akt2* expression/HOMA index in multiple linear regression analysis

	β	p *	Partial r^2 (%)
HOMA index	-0.090	0.006	11.3
BMI (kg/m^2)	0.024	0.151	2.2
HDL-cholesterol (mg/dL)	-0.002	0.805	0.1
DBP (mm Hg)	-0.005	0.526	0.6
Age (years)	0.016	0.028	8.8

r^2 for the total population was 23%

p values in Tables II, III, IV and V are adjusted for BMI, DBP, HDL-cholesterol and age.

Table VI: List of the 84 genes analyzed in the Insulin Signaling Pathway *RT^2 Profiler PCR Array System*

Insulin Receptor-associated Proteins:	Ins1, Insl3, Irs1, **Irs2**, Sorbs1, Igf1r, Igfbp1, Cbl, Grb10, Grb2, Dok1, Dok2, Dok3, Eif4ebp1, Frs2, Frs3, Gab1, **Nck1**, Ppp1ca, Ptpn1, Ptprf, **Shc1**
PI-3 Kinase Pathway:	Akt1, **Akt2**, Akt3, Eif2b1, Frap1, Pdpk1, Pik3ca, Pik3cb, Pik3r1, Pik3r2, **Prkcc**, **Prkci**, Prkcz, Adra1d, Bcl2l1, Dusp14, **G6pc**, **G6pc2**, Hk2, Igfbp1, Pck2, Serpine1, Srebf1, Ucp1, Vegfa
MAPK Pathway:	Araf, Braf, Dok2, Dok3, Gab1, Grb2, **Hras1**, Kras, Map2k1, Mapk1, Raf1, Rps6ka1, **Rras**, Rras2, **Shc1**, Sos1, Bcl2l1, Ercc1, Fos, Nos2, **Klf10** (Tieg1), Ucp1
Primary Target Genes for Insulin:	Cebpb, Fos, Jun, Lep, Prl
Secondary Effector Target Genes for Insulin Signaling:	Npy, Pck2, Tg
Target genes for PPARγ:	Acox1, Cfd (Adn), Cap1, Cebpb, Gpd1, Pck2, Pparg, Retn, Slc27a4
Target genes for SREBP1:	Acaca, Fbp1, **G6pc**, Gck, Pck2, Pklr
Carbohydrate Metabolism:	Fbp1, **G6pc**, Gck, Gpd1, Hk2, Ins1, Lep, Pck2, Pklr, Ppp1ca, Slc2a1, Sorbs1.
Lipid Metabolism:	**Ldlr**, Lep, Srebf1, Acox1, Slc27a4, Sorbs1, Araf, **Prkcc**, Prkci, Prkcz, Raf1, **Shc1**
Protein Metabolism:	**Dusp14**, Ppp1ca, Ptpn1, Ptprf, Akt1, **Akt2**, Akt3, Araf, Gsk3b, Igf1r, Map2k1, Mapk1, Pdpk1, Pik3ca, Pik3r1, **Prkcc**, **Prkci**, Prkcz, Raf1, Rps6ka1, Eif2b1, Eif4ebp1, Ppp1ca, **Hras1**, Prkci, Rras2, Bcl2l1, **Cebpa,** Cebpb, Dok3, Frs2, Gab1, Gck, Grb10, Grb2, Jun, **Ldlr**, Lep, **Nck1**, Nos2, Pik3r2, Serpine1, **Shc1**, Sorbs1, Sos1, Ucp1
Transcription Factors and Regulators:	Aebp1, **Cebpa**, Cebpb, Fos, Jun, Pparg, Srebf1, **Klf10** (Tieg1)
Cell Growth and Differentiation:	Gsk3b, **Hras1**, Igf2, Jun, Kras, Mapk1, **Irs2**, Lep, Nos2, Frs2, Igf1r, Igf2, Igfbp1, Lep, **Shc1**, Vegfa, **Cebpa**, Cebpb, Map2k1, Pik3r1, Pparg.

Classification in different categories as indicated by the manufacturer (SuperArray Bioscience; http://www.superarray.com/rt_pcr_product/HTML/PAMM-030A.html). Note that some genes are included in more than one category. Shown in colour are the 14 genes included in Figure II which exhibited downregulation (in red) or upregulation (in green) in the aortic arch of fat-fed *apoE$^{-/-}$Irs2$^{+/-}$* versus *apoE$^{-/-}$* mice.

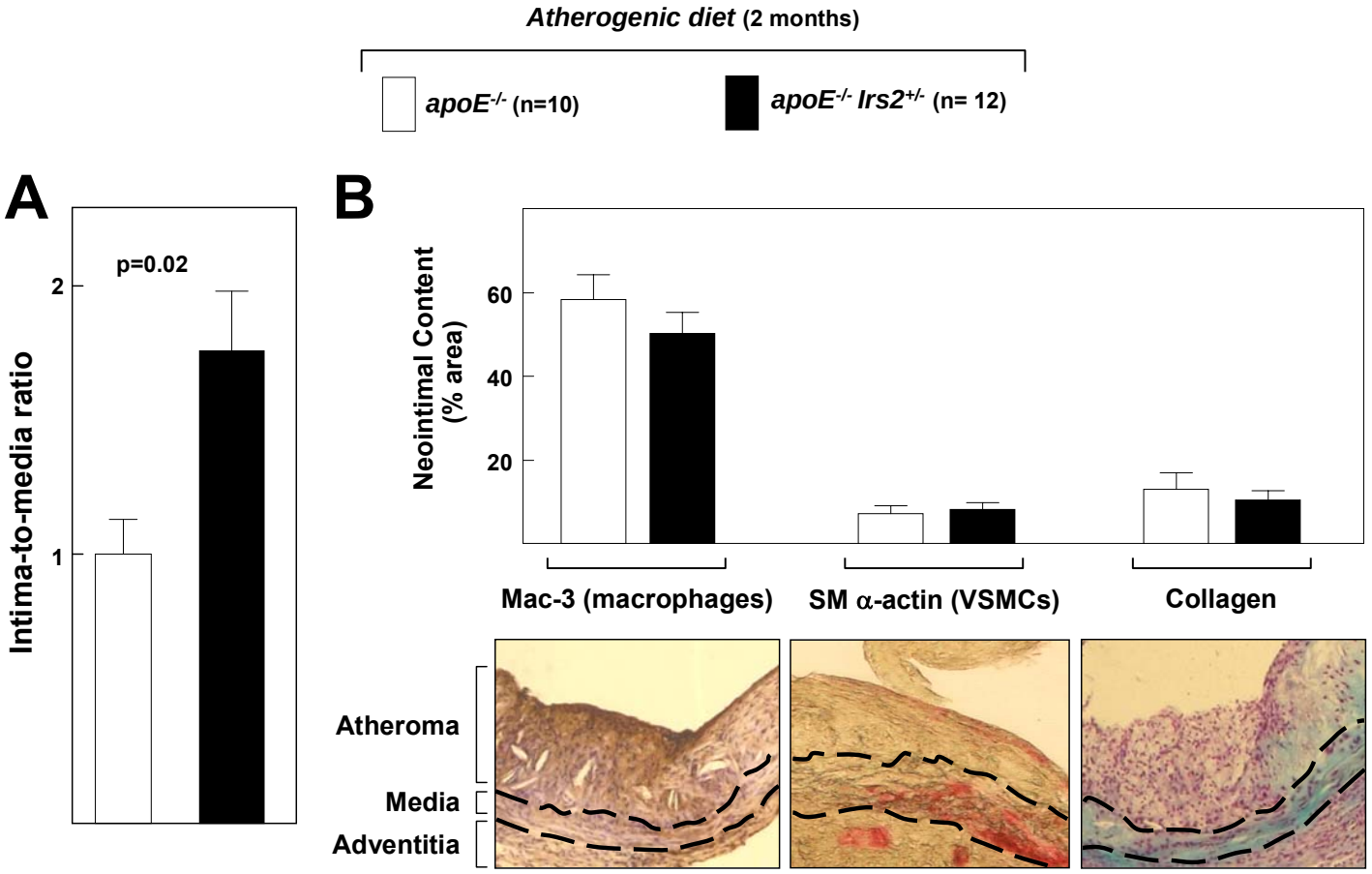

Figure I: Partial disruption of *Irs2* increases atherosclerosis burden but does not affect plaque composition. Aortic root cross-sections were obtained from mice fed the atherogenic diet for two months. **(A)** Atherosclerosis burden determined as the intima-to-media ratio. Results are expressed relative to *apoE*$^{-/-}$ mice (=1). **(B)** Neointimal content of macrophages, VSMCs and collagen was quantified using anti-Mac-3, anti-SM α–actin and Masson's Trichrome staining, respectively. Results represent the percentage of area occupied by macrophages, VSMCs and collagen versus total area of atheroma. The photomicrographs show representative images of the stainings (from *apoE*$^{-/-}$*Irs2*$^{+/-}$mice). The discontinuous lines mark the approximate contour of the tunica media. Statistically significant differences between genotypes were only observed for the intima-to-media-ratio (p=0.02, Student's t-test).

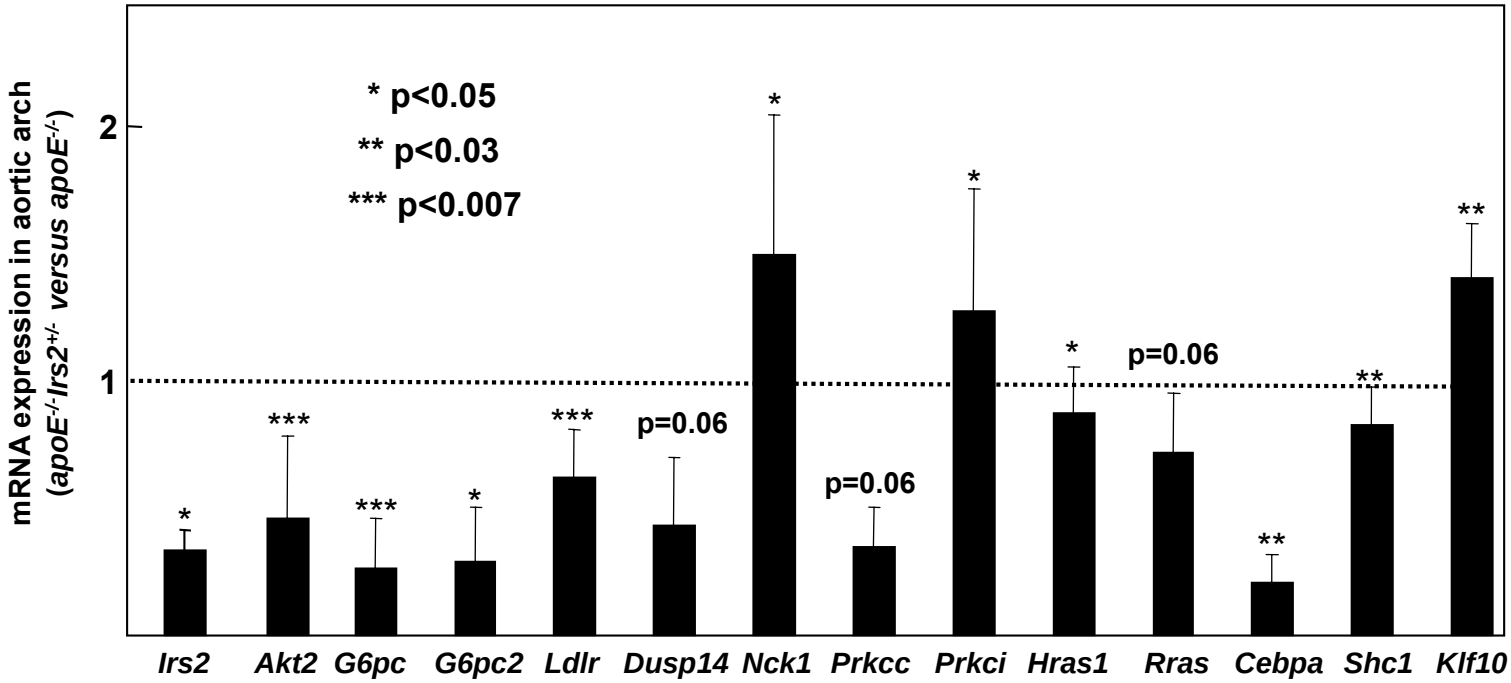

Figure II. Aortic expression of genes related to insulin signaling in fat-fed *apoE*$^{-/-}$*Irs2*$^{+/-}$ mice. Gene profiling was performed in aortic arch tissue of *apoE*$^{-/-}$ and *apoE*$^{-/-}$*Irs2*$^{+/-}$ mice fed atherogenic diet for 2 months using a murine *"Insulin signaling pathway qPCR Superarray"* system, which allow the study of 84 genes related to insulin signaling (please, see Table VI and Expanded Material and Methods in this on-line supplement). mRNA levels in *apoE*$^{-/-}$*Irs2*$^{+/-}$mice are expressed relative to *apoE*$^{-/-}$ controls (=1). Asterisks indicate genes displaying statistically significant differences between genotypes (p<0.05, Student's t-test). Three genes displayed borderline significance (p=0.06).